



HAL
open science

The glutathione peroxidase family of *Theobroma cacao*: Involvement in the oxidative stress during witches' broom disease

Akyla Maria Martins Alves, Sara Pereira Menezes Reis, Karina Peres
Gramacho, Fabienne Micheli

► To cite this version:

Akyla Maria Martins Alves, Sara Pereira Menezes Reis, Karina Peres Gramacho, Fabienne Micheli. The glutathione peroxidase family of *Theobroma cacao*: Involvement in the oxidative stress during witches' broom disease. *International Journal of Biological Macromolecules*, 2020, 164, pp.3698 - 3708. 10.1016/j.ijbiomac.2020.08.222 . hal-03491961

HAL Id: hal-03491961

<https://hal.science/hal-03491961>

Submitted on 14 Sep 2022

HAL is a multi-disciplinary open access archive for the deposit and dissemination of scientific research documents, whether they are published or not. The documents may come from teaching and research institutions in France or abroad, or from public or private research centers.

L'archive ouverte pluridisciplinaire **HAL**, est destinée au dépôt et à la diffusion de documents scientifiques de niveau recherche, publiés ou non, émanant des établissements d'enseignement et de recherche français ou étrangers, des laboratoires publics ou privés.



Distributed under a Creative Commons Attribution 4.0 International License

1 **The glutathione peroxidase family of *Theobroma cacao*: involvement in the oxidative**
2 **stress during witches' broom disease**

3

4 Akyla Maria Martins Alves¹, Sara Pereira Menezes Reis¹, Karina Peres Gramacho², Fabienne
5 Micheli^{1,3,*}

6

7 ¹Universidade Estadual de Santa Cruz (UESC), Departamento de Ciências Biológicas (DCB),
8 Centro de Biotecnologia e Genética (CBG), Rodovia Ilhéus-Itabuna, km 16, 45662-900
9 Ilhéus-BA, Brazil. E-mail: akylamma@gmail.com; menezes_sp@yahoo.com.br

10 ²Cocoa Research Center, CEPLAC/CEPEC, 45600-970 Itabuna-BA, Brasil. Email:
11 karina@cepec.gov.br

12 ³CIRAD, UMR AGAP, F-34398 Montpellier, France

13

14 ***Corresponding author:** Dr Fabienne Micheli, UESC, DCB, Rodovia Ilhéus-Itabuna km16,
15 45662-900, Ilhéus-BA, Brazil. Phone: +55 73 3680 5196. Fax: +55 73 3680 5226. E-mail:
16 fabienne.micheli@cirad.fr

17

18 **Abstract**

19 The glutathione peroxidases (GPXs) are enzymes which are part of the cell antioxidant system
20 inhibiting the ROS-induced damages of membranes and proteins. In cacao (*Theobroma cacao*
21 L.) genome, five *GPX* genes were identified. Cysteine insertion codons (UGU) were found in
22 *TcPHGPX*, *TcGPX2*, *TcGPX4*, *TcGPX6* and tryptophan insertion codon (UGG) in *TcGPX8*.
23 Multiple alignments revealed conserved domains between TcGPXs and other plants and
24 human GPXs. Homology modeling was performed using the *Populus trichocarpa* GPX5
25 structure as template, and the molecular modeling showed that TcGPXs have affinity with

26 selenomethionine in their active site. *In silico* analysis of the *TcGPXs* promoter region revealed
27 the presence of conserved *cis*-elements related to biotic stresses and hormone responsiveness.
28 The expression analysis of *TcGPXs* in cacao plantlet meristems infected by *M. perniciosa*
29 showed that *TcGPXs* are most expressed in susceptible variety than in resistant one, mainly in
30 disease stages in which oxidative stress and programmed cell death occurred. This data,
31 associated with phylogenetic and location analysis suggested that *TcGPXs* may play a role in
32 protecting cells from oxidative stress as a try of disease progression reduction. To our
33 knowledge, this is the first study of the overall GPX family from *T. cacao*.

34

35 **Keywords:** *Moniliophthora perniciosa*; programmed cell death; gene expression

36

37 1. Introduction

38 *Theobroma cacao* L. (cacao) is a plant endemic to the rainforests of South America [1]
39 and is grown mainly for the production of cocoa liquor, cocoa butter, and cocoa powder for
40 the chocolate industry [2]. However, cocoa production has been severely damaged by diseases
41 caused by fungi and oomycete [1, 3]. In Brazil, the witches' broom disease caused drastic
42 economic and social changes in the affected areas [4, 5]. This disease is caused by the
43 *Moniliophthora perniciosa* basidiomycete that presents two distinct development phases: a
44 biotrophic phase characterized by a monokaryotic and intercellular mycelium, and a
45 necrotrophic phase characterized by a dikaryotic and intracellular mycelium [6, 7]. In the
46 transition from biotrophic to necrotrophic fungal phase, the plant showed significant
47 accumulation of calcium oxalate crystals and H₂O₂, as well as events of programmed cell
48 death (PCD) [6, 8]. The accumulation of calcium oxalate causes the production of reactive
49 oxygen species (ROS) and therefore the PCD. In cacao plants susceptible to *M. perniciosa*,
50 the PCD occurs initially as a defense mechanism and then is deflected by the fungus for its
51 own benefit, allowing sporulation and further propagation [6]. The transition from the
52 biotrophic to the necrotrophic phase is facilitated by the presence of several compounds,
53 genes, and proteins that induce PCD [8, 9]. **In cacao-*M. perniciosa* interaction cDNA library
54 and/or in the cacao genome, several genes potentially related to PCD (possibly involved in its
55 enhancement or inhibition), such as the glutathione peroxidase (GPX; EC 1.11.1.9) were
56 found [10, 11].**

57 **GPXs were first discovered in mammals and** are enzymes that are part of the cell
58 antioxidant system, inhibiting the ROS-induced damage of cell membrane and proteins [12].
59 GPXs reduce H₂O₂ to water and lipid hydroperoxides to their corresponding alcohols using
60 reduced glutathione (GSH) as substrate [13]. **All mammalian GPXs contain a selenocysteine
61 (SeCys also referred to as the 21st protein amino acid) residue instead of a Cys residue [13-**

62 15]. The SeCys is encoded by an opal (TGA) stop codon, which is recognized by a special
63 transfer RNA (tRNA); the incorporation of SeCys occurs when the mRNA contains a distinct
64 hairpin mRNA sequence downstream of the UGA codon called SeCys insertion sequence
65 (SECIS) [15, 16]. It is admitted that yeast and plants do not incorporate Sec and, therefore, do
66 not have any selenoproteins [15]. However, some few studies revealed that plant kingdom
67 may also contain selenoproteins: it has been shown that in *Chlamydomonas reinhardtii*, the
68 GPX cDNA contained an internal TGA codon in frame to the ATG [17-19], in *Aloe vera*,
69 native protein purification associated to atomic absorption revealed a molecular complex of
70 four GPX subunits, each one containing one atom of selenium in its structure [20], and that in
71 cranberry, the mitochondrial genome contained two copies of selenocysteine insertion
72 sequence element (SECIS) and tRNA-Sec [21]. It has been shown that the incorporation of
73 SeCys rather than Cys in the active site of the GPX confers better redox activity to these
74 enzymes [16]. In animals, and even more in plants, only little information about the GPX
75 activity regulation is available. In animals, it has been suggested a GPX regulation at mRNA,
76 protein and/or activity level by selenium supply, SECIS-associating factors, but also by some
77 selenium-independent regulator; this regulation may also vary according to the GPX sequence
78 [22]. Some studies also pointed out the role of selenium as cofactor of GPX activity [23, 24].
79 Finally, it has also been shown the physical interaction between the human GPX1 and
80 selenium-binding protein 1 (SBP1) – which is not a selenoprotein but is able to bind selenium
81 covalently – associated to an inverse regulation of the two corresponding genes [25-27]. The
82 mechanism by which SBP1 and GPX1 regulate each other remains unclear, but a competition
83 for selenium available in the cell has been suggested as a possible mechanism of inverse
84 regulation [28]. Altogether, these data suggested a possible physical interaction between GPX
85 and selenium as possible element of activity regulation. In plants, selenium is absorbed from
86 the soil in the form of selenate (SeO_4^{2-}) or selenite (SeO_3^{2-}) that are both toxic, and are used

87 to synthesize Secys and selenomethionine (SeMet) which are further converted to volatile
88 dimethyl(di)selenide (DM(D)Se) [16]. Therefore, SeMet is one of the most abundant and
89 metabolically important forms of selenium in plant, that could be also associated to plant
90 selenium detoxification mechanism [16].

91 *GPX* gene expression has been related with cell protection in various stress conditions
92 such as pathogenic attack, salt treatment, and mechanical stimulation [29]. Interestingly, in
93 humans, the *GPx1* gene was associated to several diseases, including cancer due to disease
94 risk-associated alleles [25, 28, 30]. Several studies have also reported that HsGPx1 proteins
95 were involved in cell cycle regulation, inhibiting apoptosis that allows tumor progression [25,
96 31, 32]. For these reasons, the putative inhibitory potential of PCD associated with the ability
97 to reduce H₂O₂ and lipid hydroperoxides makes GPXs important for understanding the cacao-
98 *M. pernicioso* pathosystem. Here, we identified and analyzed *in silico* and *in vitro* five GPX
99 sequences from *T. cacao*. TcGPX proteins did not contain SeCys in their primary sequence
100 but interact with SeMet. Expression analysis of *TcGPX* genes during the cacao-*M. pernicioso*
101 interaction showed a higher expression in susceptible cacao plants than in the resistant ones,
102 mainly in disease stages in which oxidative stress and PCD occurred. This data, associated
103 with phylogenetic and location analysis suggested that *TcGPXs* may play a role in protecting
104 cells from oxidative stress, and in inhibiting PCD as a try of disease progression reduction.
105 Moreover, the *TcGPX* expression may be regulated by several hormone pathways known to
106 be involved in the witches' broom disease development, as indicated by the *TcGPX* promoter
107 analysis. To our knowledge, this is the first study of the overall GPX family from *T. cacao*.

108

109 **2. Methods**

110 **2.1 *In silico* analysis of TcGPXs**

111 A GPX cDNA was identified in a library of *T. cacao* meristem (genotype TSH1188)
112 infected by *M. perniciosa* [10]. A search in the CocoaGenDB database [11] through local
113 alignment with BLASTn and BLASTp [33] using the GPX cDNA [10] allowed the
114 identification of five homologous sequences named TcPHGPX, TcGPX2, TcGPX4, TcGPX6
115 and TcGPX8 according to the nomenclature and numeration of the cocoa genome
116 (Supplementary material 1). The complete sequences of the genes and corresponding proteins
117 were obtained from the CocoaGenDB database. The proteins were analyzed using
118 InterProScan [34] and their classification validated by the presence of the GPX domain codes.
119 The MCSanX tool [35] was used to identify possible duplications of the TcGPX genes in the
120 cacao genome. The prediction of theoretical isoelectric point (pI) and molecular weight (MW)
121 was obtained using the ExPASy Molecular Biology Server (www.expasy.org). The conserved
122 domain and family protein were analyzed using the Pfam program [36]. Post-translational
123 events were predicted using the NetPhos 2.0 Server to identify putative sites of
124 phosphorylation (Ser/Thr/Tyr) [37] and NetNGlyc 1.0 Server [38] to identify putative sites of
125 N-glycosylation. Predictions of subcellular localization were conducted with the programs
126 TargetP [39] and PSORT [40]. Signal peptide presence was analyzed using the SignalP 4.0
127 Server [41]. Homologous sequences to TcGPXs were searched using BLAST [33] on the
128 National Center for Biotechnology Information (NCBI) and plants and mammals sequences
129 showing the highest homology levels (> 79%) were selected. Multiple sequence alignment of
130 these sequences was performed with the ClustalW2 software [42], and an unrooted
131 phylogenetic tree was built using the neighbour joining method with the ClustalW2, with
132 1000 bootstraps [42] and MEGA 6 [43] programs. The search for regulatory sequences of the
133 *TcGPXs* gene was performed in the CocoaGenDB database [11]. A region of 1500 bp
134 upstream the UTR was identified and selected for *cis*-element analysis. The presence of the

135 *cis*-regulatory elements in the promoter regions of the *TcGPX* genes was analyzed using the
136 plantCARE (sphinx.rug.ac.be:8080/PlantCARE/cgi/index.html) software [44].

137

138 **2.2 Molecular modeling and docking analysis**

139 The prediction of the three-dimensional (3-D) models of the TcGPXs proteins was
140 obtained using the Swiss-Model server and the Automated Protein Homology-modeling,
141 which relies on the high similarity of target-template [45]. The crystal structure of poplar
142 (*Populus trichocarpa*) glutathione peroxidase (PtGPX5; Protein Data Bank code: 2p5q) was
143 used as the template to build the 3-D models of TcGPXs, because of its high identity with
144 TcGPXs (>79%), high coverage of protein sequences and high resolution (2.0 Å). The
145 stereochemical quality of the models was evaluated using the Procheck [46] and Anolea
146 programs [47]. The 3-D model visualization was obtained using the PyMol (The PyMOL
147 Molecular Graphics System, Version 1.5.0.4 Schrödinger, LLC.) and Discovery Studio 4.0.
148 The docking analysis between TcGPXs and SeMet was performed using the AutoDockTools
149 1.5.6 [48]. SeMet 2D structure was found in PubChem databases
150 (<http://pubchem.ncbi.nlm.nih.gov>). The 2D structure of this compound was copied into
151 Similies and saved in PDB format using the Marvin program. The ligand and receiver
152 structures were saved in pqbqt format to be used in docking calculations. AutoDock Vina was
153 used to perform Docking Scoring for the complex formed by the receptor - ligand [49]. The
154 reports of each calculation were analyzed for the energy (Kcal / Mol) values of affinity for
155 each binder conformation in its respective complex. The Discovery Studio program was used
156 to verify the ideal complex.

157

158 **2.3 Plant material**

159 Plant material was obtained as previously described [50]. Seeds of *T. cacao* genotypes
160 Catongo (susceptible to *M. perniciosa*) and TSH1188 (resistant to *M. perniciosa*) were
161 germinated and grown at CEPLAC/CEPEC (Ilhéus, Bahia, Brazil) greenhouses. Twenty to
162 thirty days after germination, the apical meristems of the plantlets were inoculated by the
163 droplet method [51] with a basidiospore suspension of *M. perniciosa* (inoculum from isolate
164 4145 maintained in the CEPLAC/CEPEC phytopathological *M. perniciosa* collection under
165 number 921 of the WFCC; <http://www.wfcc.info/index.php/collections/display>). After
166 inoculation, the plantlets were kept for 24 h at $25 \pm 2^\circ\text{C}$ and 100% humidity. Rate of disease
167 fixation based on presence/absence of symptoms [52] in each genotype, was evaluated 60
168 days after inoculation (dai); disease rate was 45% and 80% for TSH1188 and Catongo,
169 respectively. Moreover, the presence of *M. perniciosa* in the plant material was checked by
170 semi-quantitative RT-PCR using specific *M. perniciosa* actin primers [53]; both genotypes
171 presented fungus incidence (data not shown) coherent with previous data obtained in the same
172 conditions of plant culture and inoculation [7]. During the overall experiment, plant
173 development and presence/absence of symptoms were carefully checked and compared to
174 previous disease pattern established by our research group [7]. Apical meristems were
175 harvested at 24, 48 and 72 hours after inoculation (hai), and 8, 15, 30, 45, 60 and 90 dai. Non-
176 inoculated plants (controls) were kept and harvested under the same conditions at 24 and 72
177 hai, and 30 and 90 dai. Samples were collected at the same time of day (i.e. time of the
178 inoculation) to avoid possible fluctuation due to circadian rhythm. For each genotype and at
179 each harvesting time (for inoculated and non-inoculated plants), 20 samples were collected (1
180 sample = 1 apical meristem of 1 cacao plantlet). The 20 samples collected from one genotype
181 at one harvesting time were pooled; thus 9 inoculated and 5 non inoculated (control) samples
182 were immediately frozen in liquid nitrogen and stored at -80°C until use. Pooling samples

183 before RNA extraction has the advantage of reducing the variation caused by biological
184 replication and sample handling [54].

185

186 **2.4 Reverse transcription quantitative PCR analysis**

187 Samples were ground on liquid nitrogen until obtaining a fine powder. Total RNA was
188 extracted from powdered samples using the RNAqueous Kit® (Ambion) according to the
189 manufacturer's instructions, with modifications as previously described [50]. The RNA
190 quality and quantity were checked using the Nanodrop 2000 spectrophotometer (Thermo
191 Scientific). The synthesis of the first cDNA strand was carried out using Revertaid First
192 Strand cDNA Synthesis Kit according to the manufacturer's instructions (Thermo Scientific).
193 For the qPCR analysis, two cacao endogenous reference genes were used: the malate
194 dehydrogenase (MDH) and β -actin (ACT), previously identified as *T. cacao* housekeeping
195 genes [55] and tested in our experimental conditions (same plant material, same equipment)
196 [50]. Specific primers and amplified regions containing different size, melting temperature,
197 GC content and GC/AT ratio were defined to avoid cross-reaction between genes from cacao
198 *GPX* family (Supplementary material 2). The expression analysis of *TcPHGPx* and *TcGPx2*
199 was performed using standard settings of the ABI PRISM 7500 and Sequence Detection
200 System (SDS) software, version 1.6.3 (Applied Biosystems).

201 The qPCR reaction consisted of 10 ng/ μ l of cDNA, 1 μ M of each primer from
202 reference or targets genes (Supplementary material 2) and 11 μ l of Power SYBR Green
203 Master Mix (Applied Biosystems) in a total volume of 22 μ l. Cycling conditions were: 50°C
204 for 2 min then 95°C for 10 min, followed by 40 cycles at 95°C for 15 s, 60°C for 1 min and
205 72°C for 30 s. To verify that each primer pair produced only a single PCR product, a
206 dissociation analysis was carried out from 60°C to 95°C and analyzed with the Dissociation
207 Curve 1.0 program (Applied Biosystems). The expression analysis of *TcGPXs* in meristems of

208 cacao plantlets inoculated or not with *M. perniciosa*, was obtained by RT-qPCR using 3
209 experimental replicates. The relative expression was obtained using the comparative Ct
210 method ($2^{-\Delta\Delta C_t}$) that considered: i) MDH and ACT as endogenous reference genes (average of
211 expression values from both genes); and ii) non-inoculated (control) plants (average of
212 expression values of each *TcGPX* gene in 5 control samples harvested as described above) as
213 calibrator - for this reason the relative expression value of the control (= non-inoculated
214 plants) is always 1.0. Statistical analysis was made using the SASM-Agri software [56] which
215 tested the experiments as a completely randomized design. *t*-test and *F*-test (ANOVA) were
216 applied with a critical value of 0.01. The Scott-Knott ($P \leq 0.01$) test was employed for mean
217 separation when *F*-values were significant.

218

219 **3. Results**

220 **3.1 *In silico* analysis of GPX family of *T. cacao***

221 *In silico* analysis on CocoaGenDB revealed the presence of five sequences encoding
222 one *TcPHGPx* and four *TcGPXs* (*TcGPX2*, *TcGPX4*, *TcGPX6* and *TcGPX8*) (Fig. 1). *TcGPX*
223 genes were located on four different chromosomes (chromosome 1/*TcGPX4*, chromosome
224 3/*TcGPX6* and *TcGPX8*, chromosome 9/*TcPHGPX* and chromosome 5/*TcGPX2*; Fig. 1A). No
225 duplication events were found for any of the *TcGPXs* (data not shown). *TcGPX* genes were
226 2,222 to 4,805 bp in length (*TcGPX6* and *TcGPX4*, respectively; Fig. 1A), all contained 6
227 exons and 5 introns (Fig. 1A), and had ORF from 516 to 789 bp (*TcGPX4* and *TcGPX2*,
228 respectively; Table 1). *TcGPXs* encoded proteins from 171 to 262 amino acids (*TcGPX4* and
229 *TcGPX2*, respectively; Table 1), with molecular weight comprised between 19175.9 and
230 29708.3 Da (*TcGPX4* and *TcGPX2*, respectively; Table 1), and putative pI from 5.27 to 9.14
231 (*TcGPX8* and *TcGPX4*, respectively; Table 1). All *TcGPXs* showed putative phosphorylation
232 (from 7 for *TcGPX4* to 22 for *TcGPX6*) and glycosylation (from 1 for *TcPHGPX* and

233 TcGPX8 to 3 for TcGPX4 and TcGPX6) sites (Table 1). The TcGPXs were predicted to be
234 located in chloroplast (TcPHGPX and TcGPX6), to be secreted (TcGPX2), or did not present
235 any defined subcellular localization (unknown for TcGPX4 and TcGPX8; Table 1). The
236 TcGPXs mature RNA showed the initiation codes (AUG) and cysteine insertion codons
237 (UGU) in TcPHGPX, TcGPX2, TcGPX4, TcGPX6 and the tryptophan insertion codon (UGG)
238 in TcGPX8 (Fig. 1B). All TcGPXs showed at least one conserved GSH domain (Fig. 1C).
239 TcGPX family showed a cysteine instead of selenocysteine on the active site of TcPHGX,
240 TcGPX2, TcGPX4 and TcGPX6 and a tryptophan on the active site of TcGPH8 instead of a
241 selenocysteine (Fig. 1C). The alignment of TcGPXs sequence using the BLASTP tool
242 revealed high identity with GPXs from other organisms (plant and mammals) and allowed the
243 identification of the conserved region containing a conserved cysteine residue in plants and
244 SeCys in mammals (Supplementary material 3). The full-length amino acid sequences of
245 plants and mammalian of GPXs available in the databases were used to build an unrooted
246 phylogenetic tree (Supplementary material 4). Plant and mammalian GPXs were separated
247 and formed two distinct branches in the tree (Fig. 2). The five TcGPXs have close
248 phylogenetic relationship with members of the same classification in other plant species (Fig.
249 2). *In silico* analysis of the TcGPXs promoter region revealed the presence of several
250 conserved *cis*-elements characteristic of different plant species (Table. 2). Elements
251 recognized by the family of WRKY transcription factors (W box) were identified in all
252 TcGPX promoters, and defense and stress responsiveness elements (TC-rich repeats) were
253 identified in TcPHGPX, TcGPX2, TcGPX6 and TcGPX8 (Table 2). Elements related to
254 response to abiotic stress or external stimuli anaerobic induction (ARE), light responsiveness
255 (BOX4), drought-inducibility (MBS), Low-temperature responsiveness (LTR) were also
256 found (Table 2). Finally, several *cis*-elements related to hormone signaling were found such
257 as abscisic acid responsiveness (ABRE), gibberellin-responsive element (GARE-motif),

258 MeJA-responsiveness (TGACG-motif), salicylic acid responsiveness, (TCA-element) and
259 auxin-responsive element (TGA-element) (Table 2).

260

261 **3.2 Homology modeling of GPXs and docking analysis**

262 The alignment of the PtGPX5 (3-D template) amino acid sequence showed 63.92%,
263 69.03%, 59.17%, 75.15% and 84.02% with TcPHGPXs, TcGPX2, TcGPX4, TcGPX6,
264 TcGPX8, respectively (Fig. 3A). The structural modeling of TcPHGPX, TcGPX4 and
265 TcGPX6 showed 8 α -helices and 6 β -strands (Fig.3B, 3D and 3E) while TcGPX2 showed 6 α -
266 helices and, 6 β -strands (Fig.3C) and TcGPX8 7 α -helices and 6 β -strands (Fig.3F). The
267 Ramachandran plots showed that 100% of the amino acids of the TcGPXs models were
268 located in the most favored regions (Supplementary material 5). The catalytic site of
269 TcPHGPX, TcGPX2, TcGPX4, and TcGPX6 contained the conserved cysteine (Cys₁₁₄, Cys₇₅,
270 Cys₄₄, and Cys₁₁₁, respectively) residue (Fig. 3A, B, C, D and E). TcGPX8 contained two
271 conserved tryptophan (W₄₄, W₁₅₁) residue (Fig. 3A and F). The docking between TcPHGPXs
272 and SeMet showed conventional hydrogen bond interactions between Lys₁₁₃, Cys₁₁₄, Thr₁₆₃
273 and, carbon hydrogen bond between Pro₁₅₁ (Fig.4A). The interaction between TcGPX4 and
274 SeMet showed conventional hydrogen bond between Gln₇₅, Ser₁₂₉, Asn₁₀₈, Arg₁₃₆ and,
275 unfavorable donor-donor between Arg₁₃₀ (Fig.4B). The interaction between TcGPX6 and
276 SeMet showed conventional hydrogen bond between Asp₁₉₆, Arg₂₁₆, Thr₂₂₁ and, unfavorable
277 donor-donor between Ala₂₁₈ (Fig.4C). The interaction between TcGPX8 and SeMet showed
278 Pi-sulfur interaction between Phe₅₈, conventional hydrogen bond between Tyr₄₅, Trp₄₄ and
279 Glu₉₇ and carbon hydrogen between Trp₁₅₁ (Fig. 4D). No interaction was observed between
280 TcGPX2 and SeMet (data not shown).

281

282 **3.3 Differential expression of TcGPXs in resistant and susceptible cacao genotypes**
283 **infected by *M. perniciosa***

284 The expression of the *TcPHGPX*, *TcGPX2*, *TcGPX4*, *TcGPX6*, and *TcGPX8* genes
285 was analyzed together for each cacao genotype, i.e. TSH1188 (resistant to witches' broom
286 disease) and Catongo (susceptible), infected or not (control) with *M. perniciosa* (Fig.5A). For
287 both genotypes and for all the harvesting points, the PCR amplification occurred at the same
288 and unique melting temperature for each gene showing that only the corresponding gene was
289 amplified (Supplementary material 6). When we analyzed the gene expression the according
290 to the disease stage (time after inoculation), we verified that, in the resistant variety, the
291 *TcPHGPX* gene did not differ significantly at 24 and 48 hai, with a small repression compared
292 to the non-inoculated control (Fig.5B). At 72 hai, the *TcPHGPX* gene becomes significantly
293 more expressed than the control (Fig.5B). At 8 and 15 dai, the expression of the *TcPHGPX*
294 gene did not differ significantly, however, they were significantly more expressed than the
295 control (Fig.5B). At 30 dai, *TcPHGPX* was significantly less expressed than the control, and
296 at 45 and 90 dai did not differ from the control (Fig.5B). At 60 dai, the *TcPHGPX* gene was
297 overexpressed in the resistant variety (Fig.5B). In the resistant variety, the *TcGPX2* gene did
298 not differ significantly from the control after 24, 48 and 72 hai, as well as after 15, 45, and 60
299 dai after inoculation (Fig.5B). At 8 dai, the *TcGPX2* gene was repressed compared to the
300 control (Fig.5B). At 30 dai, the *TcGPX2* gene was also less expressed than the control
301 (Fig.5B). At 90 dai, the *TcGPX2* gene was significantly more expressed than in the non-
302 inoculated control (Fig.5B). The *TcGPX4* gene was only significantly more expressed than
303 the control at 60 and 90 dai (Fig.5B). The *TcGPX6* gene was significantly more expressed at
304 30, 45, and 60 dai, with a peak expression of 60 dai, followed by a 90 dai repression
305 (Fig.5B). The *TcGPX8* gene was significantly more expressed than the control at 45, 60, and
306 90 dai. In the previous periods they were less expressed than the non-inoculated control

307 (Fig.5B). In the susceptible variety the *TcPHGPX* gene was overexpressed at 24 and 48 hai
308 (Fig.5C). At 72 hai and at 8 and 15 dai, the PHGPX gene was differentially less expressed
309 than the non-inoculated control (Fig.5C). At 30 and 45 dai, the *TcPHGPX* gene did not differ
310 significantly from the non-inoculated control (Fig.5C). The *TcGPX2* gene was repressed
311 within 24 hai after being overexpressed at 48 and 72 hai (Fig.5C). At 30 dai the *TcGPX2* gene
312 was less expressed than the control (Fig.5C). At 24 hai, 8, 15, and 60 dai the *TcGPX4* gene
313 did not differ from the control (Fig.5C). At 48 and 72 hai and 90 dai TcGPx4 was less
314 expressed than the control (Fig.5C). At 30 and 45 dai the *TcGPX4* gene was overexpressed
315 (Fig.5C). The *TcGPx6* gene was overexpressed at 24 hai and 30, 45 and 90 dai. At 48 and 72
316 hai and 8 and 15 dai the expression of the *TcGPX6* gene did not differ significantly from the
317 non-inoculated control. At 60 dai the *TcGPX6* gene was significantly less expressed than the
318 control (Fig.5C). The *TcGPX8* gene was overexpressed at 24 hai and 30 and 45 dai (Fig.5C).
319 It was significantly less expressed than the control at 48 and 72 hai (Fig.5C). At 60 and 90 dai
320 the *TcGPX8* gene was significantly more expressed than the control (Fig.5C).

321 When comparing the expression of the *TcGPX* family genes, we observed that in the
322 resistant variety, 24 hai there was significant difference between the *TcPHGPX* and *TcGPX8*
323 genes (Fig.5B). At 48 hai there was no significant difference between the genes of the TcGPX
324 family (Fig.5B). At 72 hai *TcPHGPX* and *TcGPX6* were significantly more expressed
325 (Fig.5B). *TcGPx4* and *TcGPx8* did not differ significantly after 72 hai (Fig.5B). At 8 dai
326 *TcPHGPX* was significantly more expressed and *TcGPX2* was less expressed (Fig.5B). At 15
327 dai there was no difference between the genes of the *TcGPX* family (Fig.5B). At 30 dai
328 *TcGPX6* was significantly more expressed, whereas *TcPHGPX* and *TcGPx2* were less
329 expressed (Fig.5B). At 43 dai *TcGPX6* and *TcGPX8* were significantly more expressed,
330 respectively (Fig.5B). After 60 dai *TcGPx6* was significantly more expressed, whereas

331 *TcGPX2* was less expressed (Fig.5B). At 90 dai the *TcGPX2*, *TcGPX4* and *TcGPX8* genes
332 were significantly more expressed than the *TcPHGPX* and *TcGPX6* genes (Fig.5B).

333 In the susceptible variety, after 24 hai the *TcPHGPX* gene was overexpressed and
334 *TcGPX2* was less expressed than the control (Fig.5C). At 48 hai *TcPHGPX* and *TcGPX2* were
335 significantly more expressed, whereas *TcGPX4*, *TcGPX6* and *TcGPX8* were less expressed
336 than the control (Fig.5C). At 8 dai *TcGPX2* and *TcGPX4* did not differ from the control,
337 whereas *TcPHGPX*, *TcGPX6* and *TcGPX8* were less expressed than the control
338 (Fig.5C). After 30 dai the *TcGPX4* and *TcGPX8* genes were overexpressed and *TcGPX2* was
339 less expressed than the control (Fig.5C). At 45 dai *TcGPX4*, *TcGPX6* and *TcGPX8* were
340 significantly more expressed than *TcPHGPX* and *TcGPX2* (Fig.5C). After 60 dai the
341 *TcPHGPX*, *TcGPX2*, and *TcGPX6* genes were less expressed than the control. The *TcGPX4*
342 and *TcGPX8* genes did not differ from the control (Fig.5C). At 90 dai the *TcGPX6* gene was
343 significantly more expressed and the *TcGPX4* gene was less expressed than the non-
344 inoculated control (Fig.5C).

345

346 **4. Discussion**

347 **4.1 TcGPX protein family did not contain SeCys but interacted *in silico* with SeMet**

348 Here, we characterized five GPXs (*TcPHGPX*, *TcGPX2*, *TcGPX4*, *TcGPX6* and
349 *TcGPX8*) sequences from *T. cacao* (Fig. 1). All the TcGPX protein, except *TcGPX8*,
350 contained a conserved GSHPX domain with conserved Cys residues (Fig. 1C), which are
351 important for the protein function [13]. Even if it has been related in few studies the possible
352 existence of selenoproteins in plants [17, 20, 21], our results corroborate the difference
353 already observed in most of the cases between GPXs from plants and animals: the active site
354 of plant GPXs contains a Cys while the one of animal GPXs contains SeCys [57]. In the case
355 of *TcGPX8*, the Cys residue was substituted by a tryptophan residue within the GSHPX

356 domain. Although tryptophan is an amino acid with antioxidant activity [58] and could act as
357 a hydrogen donor [59], it differs greatly from the chemical structure of cysteine. It could be
358 suggested that TcGPX8 may be a non-functional GPX due to some sequence truncation or
359 mutation. On the other hand, here, we showed that TcGPXs (except TcGPX2) are able to bind
360 *in silico* the SeMet chemical element (Fig. 4). Some plant GPXs may have increased activity
361 or be selenodependent even without the presence of the UGA codon for incorporation of
362 SeCys [22, 28]. The possibility of GPXs having increased activity when interacting with
363 selenium compounds is due to the fact that selenium serves as a GPX cofactor [23, 24]. Thus,
364 as suggested here by molecular docking assays, the TcGPXs may present PCD inhibition and
365 antioxidant activities if they were associated with selenium compounds (Fig. 4).

366

367 **4.2 TcGPXs are ubiquitous protein potentially involved in cell death inhibition**

368 All the TcGPX proteins contained multiple predicted phosphorylation and
369 glycosylation sites (Table 1), which are ubiquitous mechanism for the temporal and spatial
370 regulation of proteins involved in almost every cellular process [60]. The TcGPXs family
371 showed an ubiquitous subcellular localization (Table 1) including chloroplast location
372 (TcHGPX and TcGPX6) where these proteins may use GSH or thioredoxin as a reducing
373 agent to reduce H₂O₂, organic hydroperoxide, and lipid hydroperoxides [61]. Furthermore, in
374 Arabidopsis it has been shown that chloroplastic GPXs play a role in cross talk between
375 photooxidative stress and immune responses [61, 62]. The phylogenetic analysis of TcGPXs
376 with different GPX from plants and animals showed that they were very conserved inclusive
377 for each sub-group of GPX, i.e. PHGPXs vs GPXs (Fig. 2). The sequence and structure
378 conservation of TcGPXs also suggests a conservation of function as indicated by other
379 authors [13]. In mammal signal transduction pathways, it has been suggested that PHGPx
380 functions as an anti-apoptotic agent in mitochondrial death signaling [63]. The antioxidant

381 GPX enzymes eliminate ROS and reduce H₂O₂ [64, 65] and in human, are known to be
382 inhibitors of apoptosis [66]. Functional studies of *Lycopersicon esculentum* PHGPX
383 (*LePHGPx*) showed that this gene acted as a cytoprotector in yeast, preventing Bax, hydrogen
384 peroxide, and heat stress induced cell death, but also protected tobacco leaves from salt and
385 heat stress and suppressed the apoptotic like features when expressed transiently in this plant
386 [67]. In addition, stable expression of *LePHGPx* in tobacco afforded protection against the
387 necrotrophic fungus *Botrytis cinerea* [67].

388

389 **4.3 TcGPXs may be involved in PCD reduction during *T. cacao* – *M. pernicios*** 390 **interaction**

391 The expression analysis of *TcGPX* genes by RT-qPCR in cacao plant meristems
392 infected by *M. pernicios* showed that these genes are significantly more expressed in the
393 susceptible variety than in the resistant one (Fig. 5B and C). Moreover, considering the
394 susceptible variety, *TcGPX* are most expressed during asymptomatic and green broom stages
395 (Fig.5). During dry broom phase *TcGPx6* is significantly more expressed than the other genes
396 in the susceptible variety (Fig.5C). *TcGPx2* is significantly more expressed in swelling phase
397 in susceptible variety (Fig. 5A e C). In previous works, it has been showed that calcium
398 oxalate crystal amount and H₂O₂ levels in the two cacao varieties present distinct temporal
399 and genotype dependent patterns [8]. Susceptible variety accumulated more CaOx crystals
400 than the resistant one [8, 9], the dissolution of these crystals occurred in the asymptomatic and
401 in the final stages of the disease in the resistant and the susceptible variety, respectively [8, 9].
402 Considering the role of the GPXs in the antioxidant system inhibiting the ROS-induced
403 damages, it could be suggested that in the susceptible cacao genotype infected with *M.*
404 *pernicios*, *TcGPXs* may play a role in protecting cells from oxidative stress and trying
405 reducing the progression of the disease by inhibiting PCD. Moreover, the increase of

406 *TcPHGPX* expression in susceptible variety in the initial stage of witches' broom disease may
407 be related to protection against pathogens observed in other pathosystems [67].

408 The *TcGPX* expression regulation was led by promoter regions, which contained
409 several *cis*-elements related to biotic (WRKY transcription factors) and abiotic stress (low-
410 temperature responsiveness) besides to hormone signaling such abscisic acid, gibberellin,
411 methyljasmonate-responsiveness, salicylic acid and, auxin-responsive element (Table 2).
412 Most of these hormones are involved in witches' broom disease development [10, 68-70].
413 Several genes related to plant hormone signaling were altered in cacao plants in response to
414 *M. perniciosa* infection, such ethylene-responsive element, ABA-responsive protein, auxin-
415 responsive protein, jasmonic acid 2, and brassinosteroid signalling positive regulator [10].
416 Gibberellin-responsive, ethylene biosynthesis as well as auxin-responsive genes were also
417 previously identified as up-regulated in green broom [70]. It has been suggested that the up-
418 regulation of auxin-responsive genes in infected cacao plants is a consequence of the
419 biosynthesis of this hormone by *M. perniciosa* [68-70]. In various plant pathogens, the
420 production of auxin has been correlated to the reduction of the plant defenses mediated by
421 salicylic acid, and consequently to the pathogenicity and to the biotrophic stage development
422 [68, 70].

423

424 **5. Conclusion**

425 Here we showed the first *in silico* and *in vitro* analysis of the GPX family from cacao.
426 Five *TcGPX*s sequences were analyzed at nucleotide and protein levels, and showed that the
427 ***TcGPX* proteins did** not contain SeCys in their primary sequence but interacts *in silico* with
428 SeMet as element participating of the *TcGPX* activity. This characteristic, associated to
429 phylogenetic and location analyses, suggested the participation of *TcGPX* in cell death
430 inhibition. Finally, the *TcGPX* genes were more expressed in susceptible cacao plants infected

431 by *M. pernicios* than in the resistant ones, mainly in the early disease and in the green broom
432 stages, suggesting that *TcGPXs* may play a role in protecting cells from oxidative stress, in
433 inhibiting PCD as a try of disease progression reduction. This expression may be regulated by
434 several hormone pathways known to be involved in the witches' broom disease development.

435

436 **Availability of supporting data**

437 The data sets supporting the results of this article are included within the article and its
438 additional files.

439

440 **Abbreviations**

441 ACT: actin; dai: days after inoculation; GPX: glutathione peroxidase; GSH: reduced
442 glutathione; hai: hour after inoculation; pI: isoelectric point; MDH: malate dehydrogenase;
443 MW: molecular weight; ORF: open reading frame; PCD: programmed cell death; PHGPX:
444 phospholipid hydroperoxide glutathione peroxidase; UTR: untranslated regions.

445

446 **Competing interest**

447 No conflicts of interest to declare.

448

449 **Authors' contribution**

450 AMMA was responsible for the execution of the all the experimental steps; AMMA, SPMR,
451 and FM analyzed and discussed the data; AMMA and FM wrote the manuscript; SPMR gave
452 support in qPCR experiment; KPG was responsible for plant material production and
453 inoculation with *M. pernicios*; FM and AMMA were responsible for the conception and
454 design of the experiments; FM was responsible for the financial support of the research and
455 for the advising of AMMA and SPMR.

456

457 **Acknowledgements**

458 The work of AMMA was supported by the Fundação de Amparo à Pesquisa do Estado da
459 Bahia (FAPESB). The work of SPMR was supported by the Coordenação de
460 Aperfeiçoamento de Pessoal de Nível Superior (CAPES). KPG and FM received o
461 Productivity grant from the Conselho Nacional de Desenvolvimento Científico e Tecnológico
462 (CNPq). This research was supported by the FAPESB project (DTE0038/2013) coordinated
463 by FM. The authors thank Francisca Feitosa Jucá (UESC/Ceplac) and Louise Araújo Sousa
464 (Ceplac) for technical help in plant inoculation experiments. The authors thank Raner José
465 Santana Silva (UESC) for advising in modeling, and Dr. Janisete Gomes da Silva Miller
466 (UESC) for correcting English language. This work was developed in the frame of the
467 International Consortium in Advanced Biology (CIBA; <https://www.ciba-network.org/>).

468

469 **References**

- 470 [1] G.A.R. Wood, R.A. Lass, Cocoa, Fourth Edition ed., Blackwell Science Ltd.1985.
471 [2] E.O. Afoakwa, A. Paterson, M. Fowler, A. Ryan, Flavor formation and character in cocoa and
472 chocolate: a critical review, *Crit Rev Food Sci Nutr* 48(9) (2008) 840-57.
473 [3] F. Micheli, M. Guiltinan, K.P. Gramacho, M.J. Wilkinson, A.V.d.O. Figueira, J.C.d.M. Cascardo, S.
474 Maximova, C. Lanaud, Chapter 3 - Functional genomics of cacao, in: K. Jean-Claude, D. Michel (Eds.),
475 *Advances in Botanical Research*, Academic Press2010, pp. 119-177.
476 [4] H.M. Rocha, R.A.C. Miranda, R.B. Sgrillo, R.A. Setubal, Witches' broom in Bahia, Brazil., in: S.A.
477 Rudgard, M. A.C., A. T. (Eds.), *Disease and management in Cocoa : Comparative epidemiology of*
478 *witches' broom*, Chapman and Hall, London, 1993, pp. 189-200.
479 [5] L.W. Meinhardt, J. Rincones, B.A. Bailey, M.C. Aime, G.W. Griffith, D. Zhang, G.A. Pereira,
480 *Moniliophthora perniciosa*, the causal agent of witches' broom disease of cacao: what's new from
481 this old foe?, *Molecular Plant Pathology* 9(5) (2008) 577-88.
482 [6] O. Garcia, J.A. Macedo, R. Tiburcio, G. Zapparoli, J. Rincones, L.M. Bittencourt, G.O. Ceita, F.
483 Micheli, A. Gesteira, A.C. Mariano, M.A. Schiavinato, F.J. Medrano, L.W. Meinhardt, G.A. Pereira, J.C.
484 Cascardo, Characterization of necrosis and ethylene-inducing proteins (NEP) in the basidiomycete
485 *Moniliophthora perniciosa*, the causal agent of witches' broom in *Theobroma cacao*, *Mycol Res*
486 111(Pt 4) (2007) 443-55.
487 [7] K. Sena, L. Alemanno, K.P. Gramacho, The infection process of *Moniliophthora perniciosa* in cacao,
488 *Plant Pathology* (2014) 1272–1281.
489 [8] C.V. Dias, J.S. Mendes, A.C. dos Santos, C.P. Pirovani, A. da Silva Gesteira, F. Micheli, K.P.
490 Gramacho, J. Hammerstone, P. Mazzafera, J.C. de Mattos Cascardo, Hydrogen peroxide formation in
491 cacao tissues infected by the hemibiotrophic fungus *Moniliophthora perniciosa*, *Plant Physiol*
492 *Biochem* 49(8) (2011) 917-922.

493 [9] G. de Oliveira Ceita, J.N.A. Macêdo, T.B. Santos, L. Alemanno, A. da Silva Gesteira, F. Micheli, A.C.
494 Mariano, K.P. Gramacho, D. da Costa Silva, L. Meinhardt, P. Mazzafera, G.A.G. Pereira, J.C. de Mattos
495 Cascardo, Involvement of calcium oxalate degradation during programmed cell death in *Theobroma*
496 *cacao* tissues triggered by the hemibiotrophic fungus *Moniliophthora perniciosa*, *Plant Sci* 173(2)
497 (2007) 106-117.

498 [10] A.S. Gesteira, F. Micheli, N. Carels, A. Da Silva, K. Gramacho, I. Schuster, J. Macedo, G. Pereira, J.
499 Cascardo, Comparative analysis of expressed genes from cacao meristems infected by
500 *Moniliophthora perniciosa*, *Ann Bot* 100(1) (2007) 129-140.

501 [11] X. Argout, J. Salse, J.-M. Aury, M.J. Guiltinan, G. Droc, J. Gouzy, M. Allegre, C. Chaparro, T.
502 Legavre, S.N. Maximova, M. Abrouk, F. Murat, O. Fouet, J. Poulain, M. Ruiz, Y. Roguet, M. Rodier-
503 Goud, J.F. Barbosa-Neto, F. Sabot, D. Kudrna, J.S.S. Ammiraju, S.C. Schuster, J.E. Carlson, E. Sallet, T.
504 Schiex, A. Dievert, M. Kramer, L. Gelly, Z. Shi, A. Berard, C. Viot, M. Boccarda, A.M. Risterucci, V.
505 Guignon, X. Sabau, M.J. Axtell, Z. Ma, Y. Zhang, S. Brown, M. Bourge, W. Golser, X. Song, D. Clement,
506 R. Rivallan, M. Tahj, J.M. Akaza, B. Pitollat, K. Gramacho, A. D'Hont, D. Brunel, D. Infante, I. Kebe, P.
507 Costet, R. Wing, W.R. McCombie, E. Guiderdoni, F. Quetier, O. Panaud, P. Wincker, S. Bocs, C.
508 Lanaud, The genome of *Theobroma cacao*, *Nat Genet* 43 (2011) 101–108.

509 [12] D. Trachootham, J. Alexandre, P. Huang, Targeting cancer cells by ROS-mediated mechanisms: a
510 radical therapeutic approach?, *Nature Reviews Drug Discovery* 8 (2009) 579.

511 [13] R. Margis, C. Dunand, F.K. Teixeira, M. Margis-Pinheiro, Glutathione peroxidase family – an
512 evolutionary overview, *FEBS Journal* 275(15) (2008) 3959-3970.

513 [14] S. Herbette, P. Roeckel-Drevet, J.R. Drevet, Seleno-independent glutathione peroxidases. More
514 than simple antioxidant scavengers, *FEBS J* 274(9) (2007) 2163-80.

515 [15] E. Zoidis, I. Seremelis, N. Kontopoulos, G.P. Danezis, Selenium-Dependent Antioxidant Enzymes:
516 Actions and Properties of Selenoproteins, *Antioxidants (Basel)* 7(5) (2018) 66.

517 [16] M. Schiavon, E.A. Pilon-Smits, The fascinating facets of plant selenium accumulation -
518 biochemistry, physiology, evolution and ecology, *New Phytol* 213(4) (2017) 1582-1596.

519 [17] L.-H. Fu, X.-F. Wang, Y. Eyal, Y.-M. She, L.J. Donald, K.G. Standing, G. Ben-Hayyim, A
520 Selenoprotein in the Plant Kingdom: MASS SPECTROMETRY CONFIRMS THAT AN OPAL CODON (UGA)
521 ENCODES SELENOCYSTEINE IN CHLAMYDOMONAS REINHARDTII GLUTATHIONE PEROXIDASE, *Journal*
522 *of Biological Chemistry* 277(29) (2002) 25983-25991.

523 [18] S.V. Novoselov, M. Rao, N.V. Onoshko, H. Zhi, G.V. Kryukov, Y. Xiang, D.P. Weeks, D.L. Hatfield,
524 V.N. Gladyshev, Selenoproteins and selenocysteine insertion system in the model plant cell system,
525 *Chlamydomonas reinhardtii*, *The EMBO Journal* 21(14) (2002) 3681-3693.

526 [19] D.Y. Lee, O. Fiehn, High quality metabolomic data for *Chlamydomonas reinhardtii*, *Plant*
527 *Methods* 4 (2008) 7-7.

528 [20] F. Sabeh, T. Wright, S.J. Norton, Purification and Characterization of a Glutathione Peroxidase
529 from the Aloe vera Plant, *Enzyme and Protein* 47 (1993) 92-98.

530 [21] D. Fajardo, B. Schlautman, S. Steffan, J. Polashock, N. Vorsa, J. Zalapa, The American cranberry
531 mitochondrial genome reveals the presence of selenocysteine (tRNA-Sec and SECIS) insertion
532 machinery in land plants, *Gene* 536(2) (2014) 336-43.

533 [22] X.G. Lei, W.H. Cheng, J.P. McClung, Metabolic regulation and function of glutathione peroxidase-
534 1, *Annu Rev Nutr* 27 (2007) 41-61.

535 [23] S. Chan, B. Gerson, S. Subramaniam, The role of copper, molybdenum, selenium, and zinc in
536 nutrition and health., *Clin Lab Med.* 18(4) (1998) 673-85.

537 [24] M. Puccinelli, F. Malorgio, B. Pezzarossa, Selenium Enrichment of Horticultural Crops, *Molecules*
538 22(6) (2017).

539 [25] W. Fang, M.L. Goldberg, N.M. Pohl, X. Bi, C. Tong, B. Xiong, T.J. Koh, A.M. Diamond, W. Yang,
540 Functional and physical interaction between the selenium-binding protein 1 (SBP1) and the
541 glutathione peroxidase 1 selenoprotein, *Carcinogenesis* 31(8) (2010) 1360-1366.

542 [26] M. Schott, M.M. de Jel, J.C. Engelmann, P. Renner, E.K. Geissler, A.K. Bosserhoff, S. Kuphal,
543 Selenium-binding protein 1 is down-regulated in malignant melanoma, *Oncotarget* 9(12) (2018)
544 10445-10456.

545 [27] F. Schild, S. Kieffer-Jaquinod, A. Palencia, D. Cobessi, G. Sarret, C. Zubieta, A. Jourdain, R. Dumas,
546 V. Forge, D. Testemale, J. Bourguignon, V. Hugouvieux, Biochemical and Biophysical Characterization
547 of the Selenium-binding and Reducing Site in Arabidopsis thaliana Homologue to Mammals
548 Selenium-binding Protein 1, *Journal of Biological Chemistry* 289(46) (2014) 31765-31776.

549 [28] E. Ansong, W. Yang, A.M. Diamond, Molecular cross-talk between members of distinct families
550 of selenium containing proteins, *Molecular nutrition & food research* 58(1) (2014) 117-123.

551 [29] W.-J. Li, H. Feng, J.-H. Fan, R.-Q. Zhang, N.-M. Zhao, J.-Y. Liu, Molecular cloning and expression of
552 a phospholipid hydroperoxide glutathione peroxidase homolog in *Oryza sativa*, *Biochimica et*
553 *Biophysica Acta (BBA) - Gene Structure and Expression* 1493(1-2) (2000) 225-230.

554 [30] A. Jerome-Morais, M.E. Wright, R. Liu, W. Yang, M.I. Jackson, G.F. Combs, A.M. Diamond, Inverse
555 Association Between Glutathione Peroxidase Activity and Both Selenium Binding Protein 1 Levels and
556 Gleason Score in Human Prostate Tissue, *The Prostate* 72(9) (2012) 1006-1012.

557 [31] C. Huang, G. Ding, C. Gu, J. Zhou, M. Kuang, Y. Ji, Y. He, T. Kondo, J. Fan, Decreased Selenium-
558 Binding Protein 1 Enhances Glutathione Peroxidase 1 Activity and Downregulates HIF-1 α to Promote
559 Hepatocellular Carcinoma Invasiveness, *Clinical Cancer Research* 18(11) (2012) 3042-3053.

560 [32] J.-Y. Jeong, J.-R. Zhou, C. Gao, L. Feldman, A.J. Sytkowski, Human selenium binding protein-1
561 (hSP56) is a negative regulator of HIF-1 α and suppresses the malignant characteristics of prostate
562 cancer cells, *BMB Reports* 47(7) (2014) 411-416.

563 [33] S.F. Altschul, T.L. Madden, A.A. Schaffer, J. Zhang, Z. Zhang, W. Miller, D.J. Lipman, Gapped
564 BLAST and PSI-BLAST: a new generation of protein database search programs, *Nucleic Acids Res*
565 25(17) (1997) 3389-402.

566 [34] E. Quevillon, V. Silventoinen, S. Pillai, N. Harte, N. Mulder, R. Apweiler, R. Lopez, InterProScan:
567 protein domains identifier, *Nucleic Acids Research* 33(suppl 2) (2005) W116-W120.

568 [35] Y. Wang, H. Tang, J.D. DeBarry, X. Tan, J. Li, X. Wang, T.-h. Lee, H. Jin, B. Marler, H. Guo, J.C.
569 Kissinger, A.H. Paterson, MCScanX: a toolkit for detection and evolutionary analysis of gene synteny
570 and collinearity, *Nucleic Acids Res* 40(7) (2012) e49-e49.

571 [36] S. El-Gebali, J. Mistry, A. Bateman, S.R. Eddy, A. Luciani, S.C. Potter, M. Qureshi, L.J. Richardson,
572 G.A. Salazar, A. Smart, E.L.L. Sonnhammer, L. Hirsh, L. Paladin, D. Piovesan, S.C.E. Tosatto, R.D. Finn,
573 The Pfam protein families database in 2019, *Nucleic Acids Research* 47(D1) (2019) D427-D432.

574 [37] N. Blom, S. Gammeltoft, S. Brunak, Sequence and structure-based prediction of eukaryotic
575 protein phosphorylation sites, *J Mol Biol* 294(5) (1999) 1351-62.

576 [38] R. Gupta, S. Brunak, Prediction of glycosylation across the human proteome and the correlation
577 to protein function, *Pac Symp Biocomput* (2002) 310-22.

578 [39] O. Emanuelsson, S. Brunak, G. von Heijne, H. Nielsen, Locating proteins in the cell using TargetP,
579 SignalP and related tools, *Nat. Protocols* 2(4) (2007) 953-971.

580 [40] K. Nakai, P. Horton, PSORT: a program for detecting sorting signals in proteins and predicting
581 their subcellular localization, *Trends in Biochemical Sciences* 24(1) (1999) 34-35.

582 [41] T.N. Petersen, S. Brunak, G. von Heijne, H. Nielsen, SignalP 4.0: discriminating signal peptides
583 from transmembrane regions, *Nat Meth* 8(10) (2011) 785-786.

584 [42] M.A. Larkin, G. Blackshields, N.P. Brown, R. Chenna, P.A. McGettigan, H. McWilliam, F. Valentin,
585 I.M. Wallace, A. Wilm, R. Lopez, J.D. Thompson, T.J. Gibson, D.G. Higgins, Clustal W and Clustal X
586 version 2.0, *Bioinformatics* 23(21) (2007) 2947-2948.

587 [43] K. Tamura, G. Stecher, D. Peterson, A. Filipski, S. Kumar, MEGA6: Molecular Evolutionary
588 Genetics Analysis Version 6.0, *Molecular Biology and Evolution* 30(12) (2013) 2725-2729.

589 [44] M. Lescot, P. Déhais, G. Thijs, K. Marchal, Y. Moreau, Y. Van de Peer, P. Rouzé, S. Rombauts,
590 PlantCARE, a database of plant *cis*-acting regulatory elements and a portal to tools for in silico
591 analysis of promoter sequences, *Nucleic Acids Research* 30(1) (2002) 325-327.

592 [45] K. Arnold, L. Bordoli, J. Kopp, T. Schwede, The SWISS-MODEL workspace: a web-based
593 environment for protein structure homology modelling, *Bioinformatics* 22(2) (2006) 195-201.

594 [46] R.A. Laskowski, M.W. MacArthur, D.S. Moss, J.M. Thornton, PROCHECK: a program to check the
595 stereochemical quality of protein structures, *Journal of Applied Crystallography* 26(2) (1993) 283-
596 291.

597 [47] F. Melo, E. Feytmans, Assessing protein structures with a non-local atomic interaction energy,
598 Journal of Molecular Biology 277(5) (1998) 1141-1152.

599 [48] M. Sanner, A.J. Olson, J.C. Spehner, Reduced Surface: an Efficient Way to Compute Molecular
600 Surfaces, Biopolymers 38(3) (1996) 305-320.

601 [49] O. Trott, A.J. Olson, AutoDock Vina: improving the speed and accuracy of docking with a new
602 scoring function, efficient optimization and multithreading, Journal of Computational Chemistry 31(2)
603 (2010) 455-461.

604 [50] S. Pereira Menezes, E. de Andrade Silva, E. Matos Lima, A. Oliveira de Sousa, B. Silva Andrade, L.
605 Santos Lima Lemos, K. Peres Gramacho, A. da Silva Gesteira, C. Pirovani, F. Micheli, The
606 pathogenesis-related protein PR-4b from *Theobroma cacao* presents RNase activity, Ca²⁺ and Mg²⁺
607 dependent-DNase activity and antifungal action on *Moniliophthora perniciosa*, BMC Plant Biol 14(1)
608 (2014) 1-17.

609 [51] G. Frias, L. Purdy, R. Schmidt, An inoculation method for evaluating resistance of cacao to
610 *Crinipellis perniciosa*, Plant Disease 79 (1995) 787-791.

611 [52] S. Silva, K. Matsuoka, Histologia da interação *Crinipellis perniciosa* em cacauzeiros suscetível e
612 resistente à vassoura de bruxa, Fitopatol. Bras. 24 (1999) 54-59.

613 [53] R.X. Santos, S.C.O. Melo, J.C.M. Cascardo, M. Brendel, C. Pungartnik, Carbon source-dependent
614 variation of acquired mutagen resistance of *Moniliophthora perniciosa*: Similarities in natural and
615 artificial systems, Fungal Genetics and Biology 45(6) (2008) 851-860.

616 [54] S. Duplessis, P.-E. Courty, D. Tagu, F. Martin, Transcript patterns associated with ectomycorrhiza
617 development in *Eucalyptus globulus* and *Pisolithus microcarpus*, New Phytologist 165(2) (2004) 599-
618 611.

619 [55] T.T. Pinheiro, C.G. Litholdo Jr., M.L. Sereno, G.A. Leal Jr., P.S.B. Albuquerque, A. Figueira,
620 Establishing references for gene expression analyses by RT-qPCR in *Theobroma cacao* tissues, Genet
621 Mol Res 10(4) (2012) 3291 - 3305.

622 [56] M.G. Canteri, R.A. Althaus, J.S. das Virgens Filho, E.A. Giglioti, C.V. Godoy, SASM-AGRI - Sistema
623 para análise e separação de médias em experimentos agrícolas pelos métodos Scott-Knott, Tukey a
624 Duncan, Revista Brasileira de Agrocomputação 1(2) (2001) 18-24.

625 [57] T.C. Stadtman, SELENOCYSTEINE, Annual Review of Biochemistry 65(1) (1996) 83-100.

626 [58] S. Katayama, Y. Mine, Antioxidative activity of amino acids on tissue oxidative stress in human
627 intestinal epithelial cell model, J Agric Food Chem 55(21) (2007) 8458-64.

628 [59] R.J. Elias, D.J. McClements, E.A. Decker, Antioxidant activity of cysteine, tryptophan, and
629 methionine residues in continuous phase beta-lactoglobulin in oil-in-water emulsions, J Agric Food
630 Chem 53(26) (2005) 10248-53.

631 [60] Samuel M. Pearlman, Z. Serber, James E. Ferrell, Jr., A Mechanism for the Evolution of
632 Phosphorylation Sites, Cell 147(4) (2011) 934-946.

633 [61] C.-Z. Zhai, L. Zhao, L.-J. Yin, M. Chen, Q.-Y. Wang, L.-C. Li, Z.-S. Xu, Y.-Z. Ma, Two Wheat
634 Glutathione Peroxidase Genes Whose Products Are Located in Chloroplasts Improve Salt and
635 H₂O₂ Tolerances in Arabidopsis, PLoS ONE 8(10) (2013) e73989.

636 [62] C.C.C. Chang, I. Slesak, L. Jordá, A. Sotnikov, M. Melzer, Z. Miszalski, P.M. Mullineaux, J.E. Parker,
637 B. Karpinska, S. Karpinski, Arabidopsis chloroplastic glutathione peroxidases play a role in cross talk
638 between photooxidative stress and immune responses, Plant Physiology 150(2) (2009) 670-683.

639 [63] K. Nomura, H. Imai, T. Koumura, T. Kobayashi, Y. Nakagawa, Mitochondrial phospholipid
640 hydroperoxide glutathione peroxidase inhibits the release of cytochrome c from mitochondria by
641 suppressing the peroxidation of cardiolipin in hypoglycaemia-induced apoptosis, The Biochemical
642 journal 351(Pt 1) (2000) 183-193.

643 [64] M.A.R. Milla, A. Maurer, A.R. Huete, J.P. Gustafson, Glutathione peroxidase genes in Arabidopsis
644 are ubiquitous and regulated by abiotic stresses through diverse signaling pathways, The Plant
645 Journal 36(5) (2003) 602-615.

646 [65] Z. Faltin, D. Holland, M. Velcheva, M. Tsapovetsky, P. Roedel-Drevet, A.K. Handa, M. Abu-Abied,
647 M. Friedman-Einat, Y. Eshdat, A. Perl, Glutathione Peroxidase Regulation of Reactive Oxygen Species
648 Level is Crucial for In Vitro Plant Differentiation, Plant and Cell Physiology 51(7) (2010) 1151-1162.

- 649 [66] R. Franco, J.A. Cidlowski, Apoptosis and glutathione: beyond an antioxidant, *Cell Death Differ*
650 16(10) (2009) 1303-1314.
- 651 [67] S. Chen, Z. Vaghchhipawala, W. Li, H. Asard, M.B. Dickman, Tomato phospholipid hydroperoxide
652 glutathione peroxidase inhibits cell death induced by Bax and oxidative stresses in yeast and plants,
653 *Plant Physiology* 135(3) (2004) 1630-1641.
- 654 [68] A. Kilaru, B.A. Bailey, K.H. Hasenstein, *Monilophthora perniciosa* produces hormones and alters
655 endogenous auxin and salicylic acid in infected cocoa leaves, *FEMS Microbiology Letters* 274(2)
656 (2007) 238-244.
- 657 [69] F.C. Chaves, T.J. Gianfagna, Necrotrophic phase of *Monilophthora perniciosa* causes salicylic
658 acid accumulation in infected stems of cacao, *Physiological and Molecular Plant Pathology* 69(1-3)
659 (2006) 104-108.
- 660 [70] P.J.P.L. Teixeira, D.P.d.T. Thomazella, O. Reis, P.F.V. do Prado, M.C.S. do Rio, G.L. Fiorin, J. José,
661 G.G.L. Costa, V.A. Negri, J.M.C. Mondego, P. Mieczkowski, G.A.G. Pereira, High-resolution transcript
662 profiling of the atypical biotrophic interaction between *Theobroma cacao* and the fungal pathogen
663 *Monilophthora perniciosa*, *The Plant Cell* 26(11) (2014) 4245-4269.

664

665
666

Table 1. Gene and protein characteristics of GPX family from *T. cacao*. nd: non determined.

Name	Predict gene data				Predict protein data					
	Identification*	Sequence start*	Sequence end*	ORF size (bp)	Size (aa)	Molecular weight (Da)	pI	Subcellular localization	Phosphorylation sites	Glycosylation sites
TcPHGPX	Tc09_p001340	728482	730367	720	239	26477.2	9.08	Chloroplast	S ₃₃ S ₃₆ S ₄₀ S ₄₃ S ₄₄ S ₅₈ S ₇₀ S ₉₆ S ₉₈ S ₁₂₂ S ₁₅₃ T ₂₀ T ₇₈ T ₈₁	N ₁₂₀
TcGPX2	Tc05_p000210	101857	104202	789	262	29708.3	9.11	Secretory	S ₃₁ S ₄₂ S ₅₇ S ₅₉ S ₆₂ S ₁₅₂ T ₄₇ T ₁₈₅ T ₂₄₆ Y ₄₄ Y ₉₂ Y ₁₄₇	N ₁₆₅ N ₂₂₇
TcGPX4	Tc01_p028750	24070592	24074869	516	171	19175.9	9.14	nd	S ₁₁ S ₂₈ S ₁₂₁ T ₁₆ T ₈₃ Y ₅₂ Y ₁₁₆	N ₅₀ N ₁₂₂ N ₁₃₄
TcGPX6	Tc03_p027320	23147873	23149733	780	235	25973.7	8.93	Chloroplast	S ₂₅ S ₂₉ S ₃₁ S ₃₂ S ₄₃ S ₅₂ S ₅₇ S ₆₃ S ₇₄ S ₇₅ S ₇₈ S ₉₅ S ₁₈₈ S ₁₈₉ S ₁₉₇ S ₂₂₅ T ₈₃ T ₂₂₁ Y ₁₁₈ Y ₁₂₈ Y ₁₆₆ Y ₁₈₃	N ₁₂ N ₁₁₇ N ₂₀₁
TcGPX8	Tc03_p027330	23150262	23153108	573	190	21600.4	5.27	nd	S ₅ S ₁₁ S ₂₈ S ₅₀ S ₁₅₉ S ₁₇₃ S ₁₇₆ T ₁₆ T ₅₄ Y ₁₃ Y ₆₉ Y ₇₉ Y ₁₃₄	N ₆₈

49

667

* Gene identification and position as indicated in CocoaGenDB database

668 **Table 2.** *Cis*-elements present in the promoter region of *T. cacao* GPXs genes.

Gene	Name of <i>cis</i> -elements	Organism	Function
<i>TcPHGPX</i>	ABRE	<i>Arabidopsis thaliana</i>	Abscisic acid responsiveness
	ARE	<i>Zea mays</i>	Anaerobic induction
	AT-rich	<i>Pisum sativum</i>	Maximal elicitor-mediated activation
	Box 4	<i>Petroselinum crispum</i>	Light responsiveness
	MBS	<i>Arabidopsis thaliana</i>	Drought-inducibility
	TC-rich repeats	<i>Nicotiana tabacum</i>	Defense and stress responsiveness
	W box	<i>Arabidopsis thaliana</i>	WRKY transcription factors
	ABRE	<i>Arabidopsis thaliana</i>	Abscisic acid responsiveness
<i>TcGPX2</i>	GARE-motif	<i>Brassica oleracea</i>	Gibberellin-responsive element
	MBS	<i>Arabidopsis thaliana</i>	Drought-inducibility
	TC-rich repeats	<i>Nicotiana tabacum</i>	Defense and stress responsiveness
	W box	<i>Arabidopsis thaliana</i>	WRKY transcription factors
	Box 4	<i>Petroselinum crispum</i>	Light responsiveness
	TGACG-motif	<i>Hordeum vulgare</i>	MeJA-responsiveness
	ABRE	<i>Arabidopsis thaliana</i>	Abscisic acid responsiveness
	ARE	<i>Zea mays</i>	Anaerobic induction
<i>TcGPX4</i>	Box 4	<i>Petroselinum crispum</i>	Light responsiveness
	GARE-motif	<i>Brassica oleracea</i>	Gibberellin-responsive element
	MBS	<i>Arabidopsis thaliana</i>	Drought-inducibility
	P-box	<i>Oryza sativa</i>	Gibberellin-responsive element
	TCA-element	<i>Nicotiana tabacum</i>	Salicylic acid responsiveness
	TGA-element	<i>Brassica oleracea</i>	Auxin-responsive element
	W box	<i>Arabidopsis thaliana</i>	WRKY transcription factors
	ABRE	<i>Arabidopsis thaliana</i>	Abscisic acid responsiveness
	ARE	<i>Zea mays</i>	Anaerobic induction
	Box 4	<i>Petroselinum crispum</i>	Light responsiveness
<i>TcGPX6</i>	LTR	<i>Hordeum vulgare</i>	Low-temperature responsiveness
	TC-rich repeats	<i>Nicotiana tabacum</i>	Defense and stress responsiveness
	TGA-element	<i>Brassica oleracea</i>	Auxin-responsive element
	TGACG-motif	<i>Hordeum vulgare</i>	MeJA-responsiveness
	W box	<i>Arabidopsis thaliana</i>	WRKY transcription factors
	ABRE	<i>Arabidopsis thaliana</i>	Abscisic acid responsiveness
	ARE	<i>Zea mays</i>	Anaerobic induction
	Box 4	<i>Petroselinum crispum</i>	Light responsiveness
	AT-rich	<i>Pisum sativum</i>	Maximal elicitor-mediated activation
	MBS	<i>Arabidopsis thaliana</i>	Drought-inducibility
<i>TcGPX8</i>	O2-site	<i>Zea mays</i>	Zein metabolism regulation
	TATC-box	<i>Oryza sativa</i>	Gibberellin-responsiveness
	TC-rich repeats	<i>Nicotiana tabacum</i>	Defense and stress responsiveness
	TCA-element	<i>Brassica oleracea</i>	Salicylic acid responsiveness
	TGA-element	<i>Brassica oleracea</i>	Auxin-responsive element
	W box	<i>Arabidopsis thaliana</i>	WRKY transcription factors

669

670

671 **Figure legends**

672 **Figure 1.** Schematic illustration of the genes, mature RNA and proteins of the GPX
673 family from *Theobroma cacao*. **A.** DNA sequences of GPX family. Untranslated
674 regions, exons and introns are indicated by turquoise, green and salmon squares,
675 respectively. **B.** Mature RNAs from the *TcGPX* genes. Untranslated regions and exons
676 are indicated by turquoise and green squares, respectively. Purple lines represent the
677 initiation codons (AUG), red lines indicate the cysteine insertion codons (UGU) in
678 *PHGPX*, *GPX2*, *GPX4*, *GPX6* and the tryptophan insertion codon (UGG) in *GPX8*, and
679 black lines indicate the stop codons (UGA). **C.** TcGPX protein structure. Black squares
680 represent the conserved GSH domain and yellow lines indicate the presence of cysteine
681 on the active site of TcPHGX, TcGPX2, TcGPX4 and TcGPX6, and of tryptophan on
682 the active site of TcGPX8, instead of selenocysteine.

683 **Figure 2.** Phylogenetic relationships among the nucleotide sequences of TcGPXs and
684 other plants and mammalian GPXs. Only complete sequences were considered. The tree
685 was constructed using the neighbour-joining method of clustalW with 1,000 bootstraps.
686 The amino acid sequences were obtained from GenBank.

687 **Figure 3.** Tridimensional structure of TcPHGPx, TcGPx2, TcGPx4, TcGPx6, and
688 TcGPx8 obtained by homology modeling with PtGPx5 from *Populus trichocarpa*
689 (2P5R.pdb). **A.** Alignment of the TcGPX with PtGPx5. Conserved substitutions,
690 identical amino acids, semi-conserved substitutions and catalytic triad are indicated in
691 grey, dark blue, light blue and purple, respectively. **B.** Secondary structure of
692 TcPHGPX. **C.** Secondary structure of TcGPX2. **D.** Secondary structure of TcGPx4. **E.**
693 Secondary structure of TcGPx6. **F.** Secondary structure of TcGPx8. **B-F.** The catalytic
694 triad of each TcGPx is represented by a solvent surface.

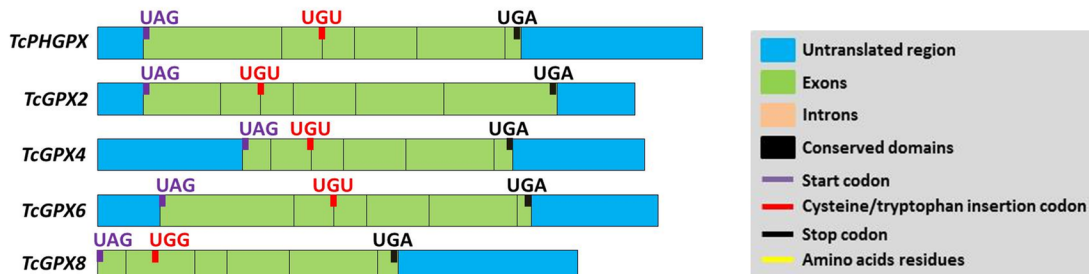
695 **Figure 4.** Docking between TcGPXs and selenomethionine (SeMet). **A.** Interaction
696 between TcPHGPX (blue) and SeMet. **B.** Interaction between TcGPX4 (orange) and
697 SeMet. **C.** Interaction between TcGPX6 (pink) and SeMet. **D.** Interaction between
698 TcGPX8 (salmon) and SeMet.

699 **Figure 5.** Relative expression of *TcPHGPX*, *TcGPX2*, *TcGPX4*, *TcGPX6*, and *TcGPX8*
700 in cacao meristems inoculated or not (control) with *M. perniciosa*. **A.** Representation of
701 plant symptoms and fungus phase during the infection time course in Catongo
702 genotypes. The harvesting times of inoculated plants are indicated on the top of the
703 figure. **B.** Relative expression observed in TSH1188. **C.** Relative expression observed in
704 Catongo. (*) indicates harvesting times of non-inoculated (control) plants. The control,
705 used as calibrator (for this reason is always 1), corresponds to the average of the
706 expression values of each *TcGPX* in 5 non-inoculated samples in each genotype (see
707 also Material and methods section). Different letters indicate significant statistical
708 difference between samples by the Scott-Knott test ($p \leq 0.01$). *t*-test was applied with a
709 critical value of 0.01: upper case letters correspond to statistics between each of the
710 genes on different harvesting times for each genotype while lower case letters
711 correspond to statistics among the genes for each harvesting time. hai: hours after
712 inoculation; dai: days after inoculation.

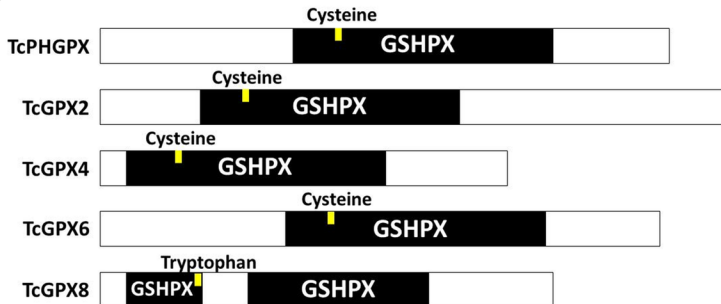
A DNA



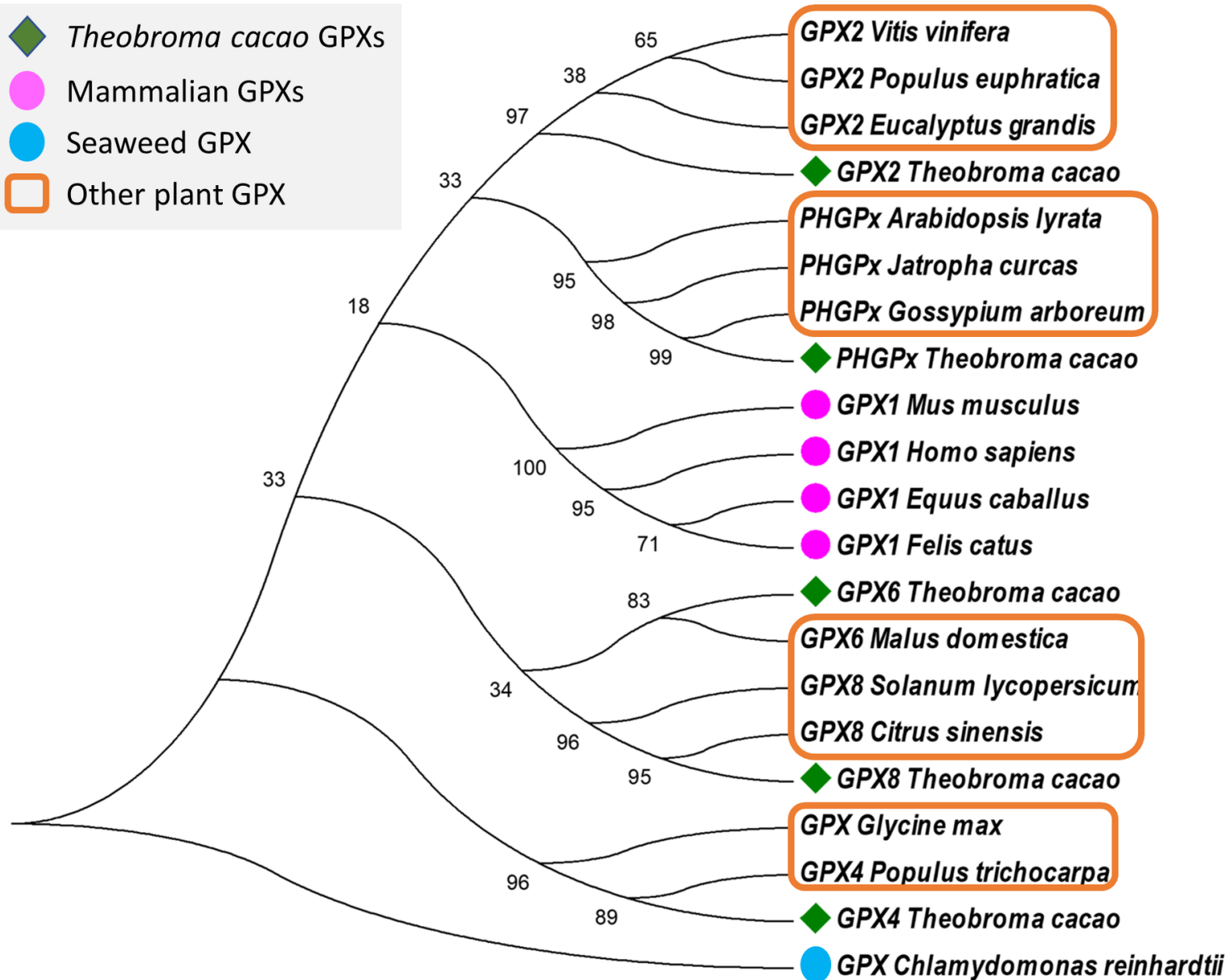
B Mature RNA



C Protein



- ◆ *Theobroma cacao* GPXs
- Mammalian GPXs
- Seaweed GPX
- Other plant GPX



A

```

TcGXP2 -----MMHRL-----FT-
TcPHGFX MASMFPSATFPFSYLHD-----LSQ--TKKIPVMPSSWPF--SIPSIES
TcGFX4 -----
TcGFX6 -----MLCSPTYLFRNRLSAVAVASLILLKRLSPSSKQTLTLLFPQISFVSLVSPSIET
TcGFX8 -----
PtGFX5 -----

TcGXP2 -----NLVLSLVLGFVFAFFLYFHYPSSSHQMAENAPKSVYEFVVKDVRGN
TcPHGFX SLGSSKSGFLQHGFLQSSSVPGFVFKSRS---SGIY--ARAATEKTLIDYVVKDIDGK
TcGFX4 -----MGASEVFPQKSLHGFVVKDNRGQ
TcGFX6 GFSRSFLGSL-----RF---DHIMAGQS--SKGSIHDFVVKDARGN
TcGFX8 -----MASQSTKNPESIIDFVVKDAJGN
PtGFX5 -----MATQTSKNPESVHDFVVKDAJEN

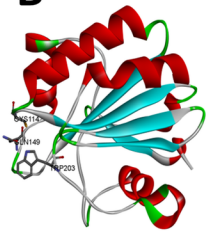
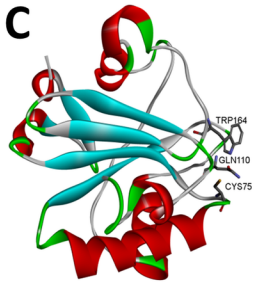
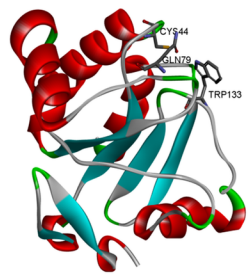
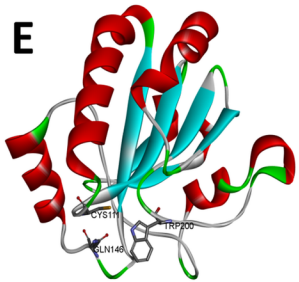
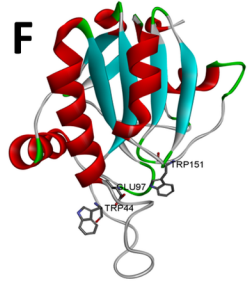
TcGXP2 DVVLSLSEYSGKVLIVNVASK-----GFTSNYSELNVLGKPKKQG
TcPHGFX DVVLSLSEYSGKVLIVNVASK-----GFTSNYSELNVLGKPKKQG
TcGFX4 DVVLSLSEYSGKVLIVNVASK-----GFTSNYSELNVLGKPKKQG
TcGFX6 DVVLSLSEYSGKVLIVNVASK-----GFTSNYSELNVLGKPKKQG
TcGFX8 VVLSLSEYSGKVLIVNVASK--YLRSDSVINTGRLLFFAT--GFTSNYSELNVLGKPKKQG
PtGFX5 DVVLSLSEYSGKVLIVNVASK-----GFTSNYSELNVLGKPKKQG

TcGXP2 LELLAPFCNQFAG--EPCSTNEHIQEVACRFFKSEPIFDKVDVNGKNSRLLKRLKLSVKGG
TcPHGFX LELLAPFCNQFGG--EPCSNPEIKQFACRFFKSEPIFDKVDVNGPNTAEVYQILAKSNAGG
TcGFX4 LELLAPFCNQFLK--EPCSTNEHQVQFACRFFKSEPIFDKVDVNGPKTESEVYKILAKSNKSG
TcGFX6 LELLAPFCNQFGG--EPCSTNEIILEFACRFFKSEPIFDKVDVNGEKTAIDIKLAKSNKSGG
TcGFX8 LELLAPFCNQFGE--EPCSTNDQIAVFCRFFKSEPIFDKVDVNGENASRLKRLKLGKVG
PtGFX5 LELLAPFCNQFGE--EPCSTNDQITDFVCRFFKSEPIFDKVDVNGENASRLKRLKLGKVG

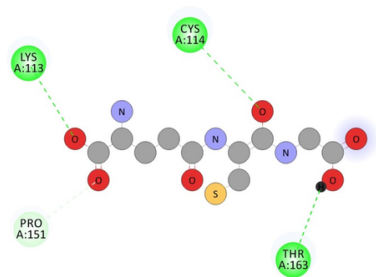
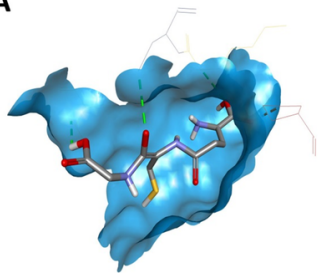
TcGXP2 YFGDAIKNEAKFLVQKGCWVRRVAFETSPKIKIQRTRDIANWFQGVHSGKAWLVFGGL
TcPHGFX FLGDLVKNEAKFLVQKGCWVRRVAFETSPKIQEKDIQKLLAA-----
TcGFX4 FLGDSIKNEAKFLVQKGCWVLRGCPPTAFALADIDIKKALGVDT-----
TcGFX6 LFGDSIKNEAKFLVQKGCWVDRVAFETSPKIDIKKLLA-----
TcGFX8 IFGDDIQNEAKFLVQKGCWVRRVAFETSPKISLSLIDIKKLLGQGE-----
PtGFX5 IFGDDIQNEAKFLVQKGCWVDRVAFETSPKISLSLIDIKKLLSITS-----

TcGXP2 RLVVFISSLNSVSGMITSSTMNYLGCAPFTHRVGCKASKHKIICNNL 69.03%
TcPHGFX ----- 63.92%
TcGFX4 ----- 59.17%
TcGFX6 ----- 75.15%
TcGFX8 ----- 84.02%
PtGFX5 -----

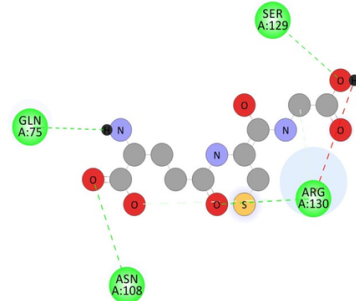
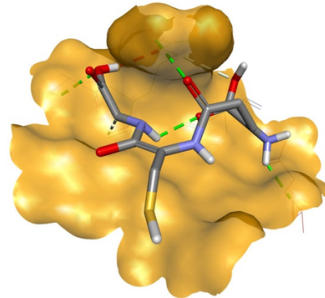
```

B**C****D****E****F**

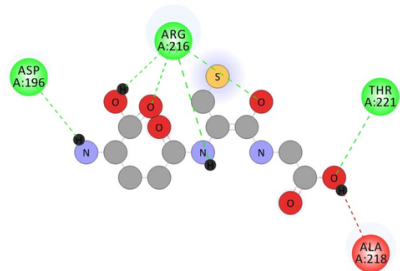
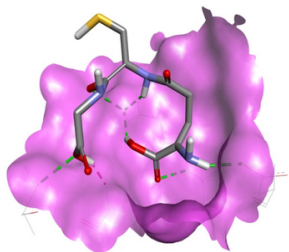
A



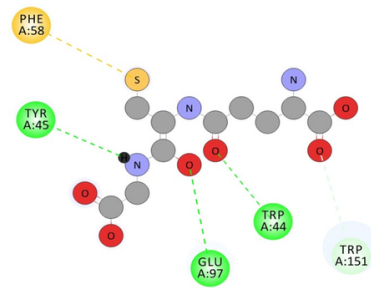
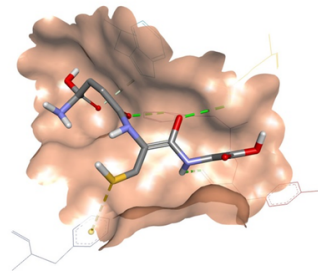
B



C



D



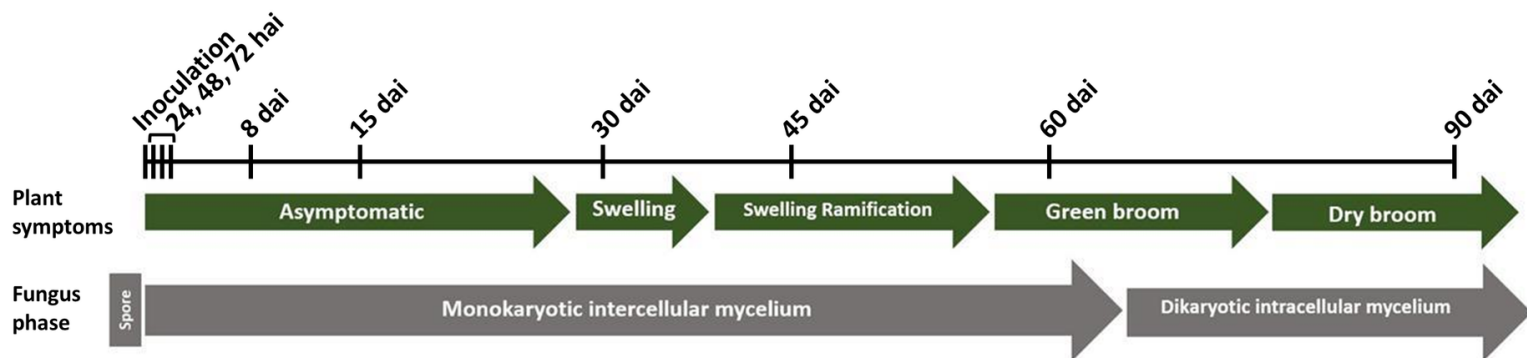
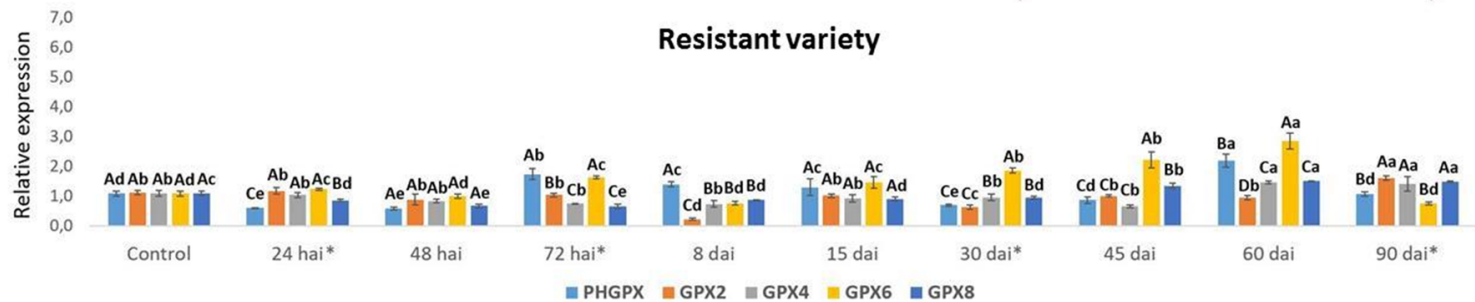
Interactions

Conventional Hydrogen Bond

Carbon Hydrogen Bond

Unfavorable Donor-Donor

Pi-Sulfur

A**B****C**